Probing quantum phases of ultracold atoms in optical lattices by transmission spectra in cavity QED

Igor B. Mekhov,[1,2,*] Christoph Maschler,[1] and Helmut Ritsch[1,†]

[1] *Institut für Theoretische Physik, Universität Innsbruck, Innsbruck, Austria*
[2] *St. Petersburg State University, V. A. Fock Institute of Physics, Department of Optics, St. Petersburg, Russia*

(Dated: February 14, 2007)

Studies of ultracold atoms in optical lattices[1] link various disciplines, providing a playground where fundamental quantum many-body concepts, formulated in condensed-matter physics, can be tested in much better controllable atomic systems[1], e.g., strongly correlated phases, quantum information processing. Standard methods to measure quantum properties of Bose-Einstein condensates (BECs) are based on matter-wave interference between atoms released from traps[2,3,4,5,6], which destroys the system. Here we propose a nondestructive method based on optical measurements, and prove that atomic statistics can be mapped on transmission spectra of a high-Q cavity. This can be extremely useful for studying phase transitions[7] between Mott insulator and superfluid states, since various phases show qualitatively distinct light scattering. Joining the paradigms of cavity quantum electrodynamics (QED) and ultracold gases will enable conceptually new investigations of both light and matter at ultimate quantum levels, which only recently became experimentally possible[8]. Here we predict effects accessible in such novel setups.

All-optical nondestructive methods to characterize atomic quantum statistics were proposed for homogeneous BECs[9,10,11,12,13]. Modified spectral properties induced by BECs were attributed to collective emission[9,10] known also for thermal atoms, to recoil[12] and local field[14] effects. Here we show a completely different phenomenon directly reflecting atom statistics in lattices due to state-dependent dispersion. For a superfluid state (SF), cavity transmission-spectra consist of numerous peaks reflecting the discreteness of the matter-field, invalidating mean-field approaches. Analogous discrete spectra reflecting the photon structure of electromagnetic fields were obtained in cavity QED with Rydberg atoms[15] and solid-state superconducting circuits[16]. A phase transition to a Mott insulator state (MI) is characterized by spectral narrowing and the degeneration to a single cavity resonance.

We consider N two-level atoms trapped in a deep optical lattice with M sites formed by strong laser beams[1]. A region of $K \leq M$ sites is illuminated by two additional light modes (Fig. 1). Although these modes could belong to a single cavity, we consider two cavities, whose geometries (i.e. axis directions or wavelengths) can be varied.

As shown in the Methods section, the Heisenberg equations for the annihilation operators of two light modes a_l ($l = 0, 1$) with frequencies ω_l and mode functions $u_l(\mathbf{r})$ are

$$\dot{a}_l = -i\left(\omega_l + \frac{g^2\hat{D}_{ll}}{\Delta_{la}}\right)a_l - i\frac{g^2\hat{D}_{lm}}{\Delta_{ma}}a_m - \kappa a_l + \eta_l(t), \quad (1)$$

$$\text{with} \quad \hat{D}_{lm} \equiv \sum_{i=1}^{K} u_l^*(\mathbf{r}_i)u_m(\mathbf{r}_i)\hat{n}_i,$$

where $l \neq m$, g is the atom-light coupling constant, $\Delta_{la} = \omega_l - \omega_a$ are the large cavity-atom detunings, κ is the cavity relaxation rate, $\eta_l(t) = \eta_l e^{-i\omega_{l_p}t}$ gives the external probe and $\hat{n}_i$ are the atom number operators at a site with coordinate $\mathbf{r}_i$. We also introduce the operator of the atom number at illuminated sites $\hat{N}_K = \sum_{i=1}^{K}\hat{n}_i$.

In a classical limit, Eq. (1) corresponds to Maxwell's equations with the dispersion frequency-shifts of cavity modes $g^2\hat{D}_{ll}/\Delta_{la}$ and the coupling coefficient between them $g^2\hat{D}_{10}/\Delta_{1a}$. A quantum treatment of those quantities as operators will lead to striking results.

From Eq. (1) one can express the light operators as some function $f(\hat{n}_1, ..., \hat{n}_M)$ of atomic operators, and then calculate their expectation values for some prescribed atomic states $|\Psi\rangle$, e.g., the MI and SF states.

The MI is a product of Fock states at all sites, $|\Psi\rangle_{\mathrm{MI}} = \prod_{i=1}^{M}|q_i\rangle_i \equiv |q_1, ..., q_M\rangle$, giving the expectation values as

$$\langle f(\hat{n}_1, ..., \hat{n}_M)\rangle_{\mathrm{MI}} = f(q_1, ..., q_M), \quad (2)$$

since $\hat{n}_i|q_1, ..., q_M\rangle = q_i|q_1, ..., q_M\rangle$. Thus, for light scattering, MI is the most classical state corresponding to pointlike atoms ($\langle\hat{n}_i\rangle_{\mathrm{MI}} = q_i$ atoms at ith site). We will consider equal average densities $\langle\hat{n}_i\rangle_{\mathrm{MI}} = N/M \equiv n$ at all sites ($\langle\hat{N}_K\rangle_{\mathrm{MI}} = nK \equiv N_K$).

In a SF sate (BEC), each atom is delocalized over all sites leading to number fluctuations at $K < M$ sites. It is given by a superposition of all multisite Fock states corresponding to all possible distributions of N atoms at M sites: $|\Psi\rangle_{\mathrm{SF}} = \sum_{q_1,...,q_M}\sqrt{N!/M^N}/\sqrt{q_1!...q_M!}|q_1, ..., q_M\rangle$ with $\sum_{i=1}^{M} q_i = N$. The density $\langle\hat{n}_i\rangle_{\mathrm{SF}} = N/M$ is identical to that in MI but light scattering will be shown to be spectrally different. Expectation values of light operators then can be calculated from

$$\langle f(\hat{n}_1, ..., \hat{n}_M)\rangle_{\mathrm{SF}} = \frac{1}{M^N}\sum_{q_1,...,q_M}\frac{N!}{q_1!...q_M!}f(q_1, ..., q_M), \quad (3)$$

representing a sum of "classical" terms given by all possible atomic distributions, which is obviously different from $\langle f(\hat{n}_1, ..., \hat{n}_M)\rangle_{\mathrm{MI}}$ (2).

In the simplest case of a single mode a_0 ($a_1 \equiv 0$), the stationary solution of Eq. (1) for the number of photons in a cavity reads

$$a_0^\dagger a_0 = f(\hat{n}_1, ..., \hat{n}_M) = \frac{|\eta_0|^2}{(\Delta_p - g^2\hat{D}_{00}/\Delta_{0a})^2 + \kappa^2}, \quad (4)$$

where $\Delta_p = \omega_{0p} - \omega_0$ is the probe-cavity detuning. We present various transmission spectra in Fig. 2 for the case, where $|u_0(\mathbf{r}_i)|^2 = 1$, and $\hat{D}_{00} = \sum_{i=1}^K \hat{n}_i$ reduces to $\hat{N}_K$. For a 1D lattice (see Fig. 1), this occurs in the cases of a traveling wave at any angle to the lattice, and standing wave transverse ($\theta_0 = \pi/2$) or parallel ($\theta_0 = 0$) to the lattice with atoms trapped at field maxima.

For MI (see Eq. (2)), the photon number $\langle a_0^\dagger a_0\rangle_{\rm MI}$ as a function of the detuning is a single Lorentz contour described by Eq. (4) with width κ and classical frequency shift given by $g^2\langle\hat{D}_{00}\rangle_{\rm MI}/\Delta_{0a} = g^2\sum_{i=1}^K |u_0(\mathbf{r}_i)|^2\langle\hat{n}_i\rangle/\Delta_{0a}$ (equal to g^2N_K/Δ_{0a} in Fig. 2).

In contrast, for a SF state, Eq. (3) gives a sum of Lorentzians with different dispersion shifts corresponding to all atomic distributions $|q_1, ..., q_K\rangle$. So, if each Lorentzian is resolved, one can measure a comb-like structure by scanning the probe frequency Δ_p. In Figs. 2a and 2c, the shifts correspond to all possible atom numbers at K sites (i.e. 0,1,2,...,N) separated by g^2/Δ_{0a}. For larger κ the spectrum becomes continuous (Fig. 2b), but broader than that for MI.

Scattering of weak fields does not change the atom number distribution. However, as the SF is a quantum superposition of different atom numbers in a region with K sites, a measurement projects the state into a subspace with fixed N_K in this region, and a subsequent measurement on a time scale short to tunneling between neighbour sites will yield the same result. One recovers the full spectrum of Fig. 2 by repeating the experiment or with sufficient time delay to allow for redistribution via tunneling. Such repeated measurements will allow a time dependent study of tunneling and buildup of long-range order of correlations in the lattice. Alternatively, one can continue measurements on the reduced subspace after changing a lattice region or the light geometry.

We will now consider two modes of the equal frequencies $\omega_0 = \omega_1$, the probe injected only into the mode a_0 (Fig. 1) and the mentioned geometries where the shift operators are $\hat{D}_{00} = \hat{D}_{11} = \hat{N}_K$ (see Fig. 3). From Eq. (1), the stationary photon number $a_1^\dagger a_1 = f(\hat{n}_1, ..., \hat{n}_M)$ is

$$a_1^\dagger a_1 = \frac{(g^2/\Delta_{1a})^2\hat{D}_{10}^\dagger\hat{D}_{10}|\eta_0|^2}{[\hat{\Delta}_p'^2 - (g^2/\Delta_{1a})^2\hat{D}_{10}^\dagger\hat{D}_{10} - \kappa^2]^2 + 4\kappa^2\hat{\Delta}_p'^2}, \quad (5)$$

where $\hat{\Delta}_p' = \Delta_p - g^2\hat{D}_{11}/\Delta_{0a}$.

In a classical (and MI) case, Eq. (2) gives a two-satellite contour (5) reflecting normal mode splitting of two oscillators $\langle a_{0,1}\rangle$ coupled through atoms. This was recently observed[17] for collective strong coupling, i.e., the splitting $g^2\langle\hat{D}_{10}\rangle/\Delta_{1a}$ exceeding κ. The splitting depends on the geometry through the mode functions (see Eq. (1)) representing diffraction of one mode into another. Thus, our results can be treated as light scattering from a "quantum diffraction grating" generalizing Bragg scattering, well-known in different disciplines. In diffraction maxima (i.e. $u_1^*(\mathbf{r}_i)u_0(\mathbf{r}_i) = 1$) one finds $\hat{D}_{10} = \hat{N}_K$ providing the maximal classical splitting. In diffraction minima, one finds $\hat{D}_{10} = \sum_{i=1}^K (-1)^{i+1}\hat{n}_i$ providing both the classical splitting and photon number are almost zero.

In SF, Eq. (3) shows that $\langle a_1^\dagger a_1\rangle_{\rm SF}$ is given by a sum of all possible classical terms with all possible normal mode splittings. In a diffraction maximum (Figs. 3a,b), the right satellite is split into components corresponding to all possible N_K or extremely broadened. In a minimum with $K = M$ (Figs. 3c,d), the splittings are determined by all differences between atom numbers at odd and even sites $\sum_{i=1}^K (-1)^{i+1}q_i$. Note that there is no classical description of the spectra in a minimum, since here the classical field (and $\langle a_1^\dagger a_1\rangle_{\rm MI}$) are zero for any Δ_p.

In each of the examples presented in Figs. 2 and 3, the photon number depends only on one statistical quantity q, $f(q_1, ..., q_M) = f(q)$: for a single mode and two modes in a maximum, q is the atom number at K sites; for two modes in a minimum with $K = M$, q is the atom number at odd (or even) sites. In the Methods section, we show that Eq. (3) reduces then to a simple expression $\langle f\rangle_{\rm SF} = \sum_{q=0}^N f(q)p(q)$, where $p(q)$ is the distribution function of q.

In high-Q cavities ($\kappa < g^2/\Delta_{0a}$), $f(q)$ is given by well-separated Lorentzians of widths κ peaked at Δ_p^q depending on q ($q = 0, 1, ..., N$) and amplitudes proportional to $p(q)$. Using $p(q)$, we can write the envelope of such a comb. For a single mode [Fig. 2a,c, Eq. (4)], we find $\Delta_p^q \approx g^2 q/\Delta_{0a}$ with the envelope

$$\langle a_0^\dagger a_0(\Delta_p^q)\rangle_{\rm SF} = \frac{\alpha g^2}{\sqrt{2\pi}\Delta_{0a}\sigma_\omega} e^{-(\Delta_p^q - \tilde{\Delta}_p)^2/2\sigma_\omega^2}, \quad (6)$$

where $\tilde{\Delta}_p = g^2N_K/\Delta_{0a}$, $\sigma_\omega = g^2\sqrt{N_K(1 - K/M)}/\Delta_{0a}$, and $\alpha = |\eta_0|^2/\kappa^2$. So, the spectrum envelopes in Fig. 2a,c are well described by Gaussians of widths strongly depending on K.

The atom number at K sites fluctuates in SF with the variance $(\Delta N_K)^2 = N_K(1 - K/M)$, so the spectral width can be written as $\sigma_\omega = g^2\sqrt{(\Delta N_K)^2}/\Delta_{0a}$. Thus, the atomic distribution function $p(q)$ is mapped on the light spectrum. Figure 2c shows spectra for different lattice regions demonstrating Gaussian and Poissonian distributions (see Methods). For $K \approx M$ the spectrum narrows, and for the whole lattice illuminated it should shrink to a single Lorentzian as in the MI case.

The condition $\kappa < g^2/\Delta_{0a}$ is already met in present experiments. In the recent work[8], where setups of cavity QED and ultracold gases were joined to probe quantum statistics of an atom laser with ^{87}Rb atoms, the parameters are $(g, \Delta_{0a}, \kappa) = 2\pi \times (10.4, 30, 1.4)$ MHz. The setups used for cavity cooling of atoms[18,19] are also very promising.

For bad cavities ($\kappa \gg g^2/\Delta_{0a}$), the sums can be replaced by integrals with the same parameters $\tilde{\Delta}_p$ and σ_ω as for $\kappa < g^2/\Delta_{0a}$. For example, for a single mode (Fig. 2b),

$$\langle a_0^\dagger a_0(\Delta_p)\rangle_{\rm SF} = \frac{|\eta_0|^2}{\sqrt{2\pi}\sigma_\omega}\int_0^\infty \frac{e^{-(\omega-\tilde{\Delta}_p)^2/2\sigma_\omega^2}d\omega}{(\Delta_p-\omega)^2+\kappa^2}, \quad (7)$$

representing a Voigt contour, well-know in laser spectroscopy of hot gases. Here, the inhomogeneous broadening is a striking contribution of quantum statistics.

In conclusion, we have shown that transmission spectra of light scattered from atoms in optical lattices radically differ for various atomic states. Note that such information is also contained in the amplitudes $\langle a_{0,1}\rangle$ contrasting with claims[13] that $\langle a_{0,1}\rangle$ probes only the average density. This becomes possible due to (i) orthogonality of Fock states corresponding to different atom distributions and (ii) different frequency shifts of light fields entangled to those states. In general, various optical phenomena and quantities depending nonlinearly on atom number operators should reflect atomic quantum statistics[20,21].

Acknowledgements

The work was supported by FWF (P17709 and S1512). While preparing this manuscript, we became aware of a closely related research in the group of P. Meystre. We are grateful to him for sending us the preprint[21] and stimulating discussions.

Correspondence and requests for materials should be addressed to I.B.M or H.R.

Competing financial interests

The authors declare that they have no competing financial interests.

* Electronic address: Igor.Mekhov@uibk.ac.at
† Electronic address: Helmut.Ritsch@uibk.ac.at

1 Bloch, I. Ultracold quantum gases in optical lattices. *Nat. Phys.* **1**, 23–30 (2005).
2 Fölling, S. *et al.* Spatial quantum noise interferometry in expanding ultracold atom clouds. *Nature* **434**, 481–484 (2005).
3 Altman, E., Demler, E., & Lukin, M. D. Probing many-body states of ultracold atoms via noise correlations. *Phys. Rev. A* **70**, 013603 (2004).
4 Stöferle, T., Moritz, H., Schori, C., Köhl, M. & Esslinger, T. Transition from a strongly interacting 1D superfluid to a Mott insulator. *Phys. Rev. Lett.* **92**, 130403 (2004).
5 Gritsev, V., Altman, E., Demler, E. & Polkovnikov, A. Full quantum distribution of contrast in interference experiments between interacting one-dimensional Bose liquids. *Nat. Phys.* **2**, 705–709 (2006).
6 Schellekens, M. *et al.* Hanbury Brown Twiss effect for ultracold quantum gases. *Science* **310**, 648–651 (2005).
7 Jaksch, D., Bruder, C., Cirac, J. I., Gardiner, C. W. & Zoller, P. Cold bosonic atoms in optical lattices *Phys. Rev. Lett.* **81**, 3108–3111 (1998).
8 Bourdel, T. *et al.* Cavity QED detection of interfering matter waves. *Phys. Rev. A* **73**, 043602 (2006).
9 You, L., Lewenstein, M. & Cooper, J. Line shapes for light scattered from Bose-Einstein condensates. *Phys. Rev. A* **50**, R3565–R3568 (1994).
10 Javanainen, J. Optical signatures of a tightly confined Bose condensate. *Phys. Rev. Lett.* **72**, 2375–2378 (1994).
11 You, L., Lewenstein, M., & Cooper, J. Quantum field theory of atoms interacting with photons. II. Scattering of short laser pulses from trapped bosonic atoms. *Phys. Rev. A* **51**, 4712–4727 (1995).
12 Javanainen, J. & Ruostekoski, J. Off-resonance light scattering from low-temperature Bose and Fermi gases. *Phys. Rev. A* **52**, 3033–3046 (1995).
13 Parkins, A. S. & Walls, D. F. The physics of trapped dilute-gas Bose-Einstein condensates. *Phys. Rep.* **303**, 1-80 (1998).
14 Morice, O., Castin, Y. & Dalibard, J. Refractive index of a dilute Bose gas. *Phys. Rev. A* **51**, 3896–3901 (1995).
15 Brune, M., *et al.* Quantum Rabi oscillation: a direct test of field quantization in a cavity. *Phys. Rev. Lett.* **76**, 1800–1803 (1996).
16 Gambetta, J. *et al.* Qubit-photon interactions in a cavity: Measurement-induced dephasing and number splitting. *Phys. Rev. A* **74**, 042318 (2006).
17 Klinner, J., Lindholdt, M., Nagorny, B. & Hemmerich, A. Normal mode splitting and mechanical effects of an optical lattice in a ring cavity. *Phys. Rev. Lett.* **96**, 023002 (2006).
18 Maunz, P. *et al.* Cavity cooling of a single atom. *Nature* **428**, 50–52 (2004).
19 Hood, C. J., Lynn, T. W., Doherty, A. C., Parkins, A. S. & Kimble, H. J. The atom-cavity microscope: single atoms bound in orbit by single photons. *Science* **287**, 1447–1453 (2000).
20 Mekhov, I. B., Maschler, C. & Ritsch, H. Cavity enhanced light scattering in optical lattices to probe atomic quantum satistics. quant-ph/0610073.
21 Chen, W., Meiser, D. & Meystre, P. Cavity QED determination of atomic number statistics in optical lattices. quant-ph/0610029.
22 Maschler, C. & Ritsch, H. Cold atom dynamics in a quantum optical lattice potential. *Phys. Rev. Lett.* **95**, 260401 (2005).
23 Slama, S., von Cube, C., Kohler, M., Zimmermann, C. & Courteille, P. V. Multiple reflections and diffuse scattering in Bragg scattering at optical lattices. *Phys. Rev. A* **73**, 023424 (2006).

Methods

Derivation of Heisenberg equations

A manybody Hamiltonian for our system presented in Fig. 1 is given by

$$H = \sum_{l=0,1} \hbar\omega_l a_l^\dagger a_l + \int d^3\mathbf{r}\Psi^\dagger(\mathbf{r}) H_{a1} \Psi(\mathbf{r}), \text{with}$$

$$H_{a1} = \frac{\mathbf{p}^2}{2m_a} + V_{\rm cl}(\mathbf{r}) + \hbar g^2 \sum_{l,m=0,1} \frac{u_l^*(\mathbf{r}) u_m(\mathbf{r}) a_l^\dagger a_m}{\Delta_{ma}},$$

where $a_{0,1}$ are the annihilation operators of the modes of frequencies $\omega_{0,1}$, wave vectors $\mathbf{k}_{0,1}$, and mode functions $u_{0,1}(\mathbf{r})$; $\Psi(\mathbf{r})$ is the atom-field operator. In the effective single-atom Hamiltonian H_{a1}, $\mathbf{p}$ and $\mathbf{r}$ are the momentum and position operators of an atom of mass m_a trapped in the classical potential $V_{\rm cl}(\mathbf{r})$, and g is the atom–light coupling constant. We consider off-resonant scattering where the detunings between fields and atomic transition $\Delta_{la} = \omega_l - \omega_a$ are larger than the spontaneous emission rate and Rabi frequencies. Thus, in H_{a1} the adiabatic elimination of the upper state, assuming linear dipoles with adiabatically following polarization, was used.

For a one-dimensional lattice with period d and atoms trapped at $x_j = jd$ $(j = 1, 2, \ldots, M)$ the mode functions are $u_{0,1}(\mathbf{r}_j) = \exp(ijk_{0,1x}d + i\phi)$ for traveling and $u_{0,1}(\mathbf{r}_j) = \cos(jk_{0,1x}d + i\phi)$ standing waves with $k_{0,1x} = |\mathbf{k}_{0,1}|\cos\theta_{0,1}$, $\theta_{0,1}$ are angles between the mode and lattice axes, ϕ is some spatial phase shift (cf. Fig. 1).

Assuming the modes $a_{0,1}$ much weaker than the trapping beam, we expand $\Psi(\mathbf{r})$ using localized Wannier functions[7] corresponding to the potential $V_{\rm cl}(\mathbf{r})$ and keep only the lowest vibrational state at each site: $\Psi(\mathbf{r}) = \sum_{i=1}^{M} b_i w(\mathbf{r} - \mathbf{r}_i)$, where b_i is the annihilation operator of an atom at site i at a position $\mathbf{r}_i$. Substituting this expansion in the Hamiltonian H, one can get a generalized Bose-Hubbard model[7] including light scattering. In contrast to "Bragg spectroscopy", which involves scattering of matter waves[4], and our previous work[22], we neglect lattice excitations here and focus on light scattering from atoms in some prescribed quantum states.

Neglecting atomic tunneling, the Hamiltonian reads:

$$H = \sum_{l=0,1} \hbar\omega_l a_l^\dagger a_l + \hbar g^2 \sum_{l,m=0,1} \frac{a_l^\dagger a_m}{\Delta_{ma}} \left(\sum_{i=1}^{K} J_{i,i}^{lm} \hat{n}_i \right),$$

where $\hat{n}_i = b_i^\dagger b_i$. For deep lattices the coefficients $J_{i,i}^{lm} = \int d\mathbf{r} w^2(\mathbf{r} - \mathbf{r}_i) u_l^*(\mathbf{r}) u_m(\mathbf{r})$ reduce to $J_{i,i}^{lm} = u_l^*(\mathbf{r}_i) u_m(\mathbf{r}_i)$ neglecting spreading of atoms, which can be characterized even by classical scattering[23]. The Heisenberg equations obtained from this Hamiltonian are given by Eq. (1).

Simple expressions for spectral line shapes

We will now present the derivation of Eqs. (6) and (7) demonstrating relations between atomic quantum statistics and the transmission spectra. As has been mentioned in the main text, in all examples presented in Figs. 2 and 3, the photon number depends only on a single statistical quantity q. Using this fact, the multinomial distribution in Eq. (3) reduces to a binomial, which can be directly derived from Eq. (3): $\langle f \rangle_{\rm SF} = \sum_{q=0}^{N} f(q) p(q)$ with $p(q) = N!/[q!(N-q)!](Q/M)^q (1 - Q/M)^{N-q}$ and a single sum instead of M ones. Here Q is the number of specified sites: Q is equal to K for one mode and two modes in a maximum; Q is the number of odd (or even) sites for two modes in a minimum ($Q = M/2$ for even M). This approach can be used for other geometries, e.g., for two modes in a minimum and $K < M$, where Eq. (3) can be reduced to a trinomial distribution.

As a next approximation we consider $N, M \gg 1$, but finite N/M, leading to the Gaussian distribution $p(q) = 1/(\sqrt{2\pi}\sigma_q) \exp\left[-(q - \tilde{q})^2/2\sigma_q^2\right]$ with central value $\tilde{q} = NQ/M$ and width $\sigma_q = \sqrt{N(Q/M)(1 - Q/M)}$.

Using this Gaussian distribution, Eq. (6) was obtained as an envelope of Lorentzians in the case of a single mode (Fig. 2a). For $K \to 0$ and $K \to M$, the binomial distribution $p(q)$ is well approximated by a Poissonian distribution, which is demonstrated in Fig. 2c for $K = 10$ and $K = 68$.

In other examples (Figs. 3a and 3c), Eq. (6) is also valid, although with other parameters. For two modes in a diffraction maximum (Fig. 3a), the central frequency, separation between Lorentzians and width are doubled: $\tilde{\Delta}_p = 2g^2 N_K/\Delta_{0a}$, $\Delta_p^q \approx 2g^2 q/\Delta_{0a}$ and $\sigma_\omega = 2g^2\sqrt{N_K(1 - K/M)}/\Delta_{0a}$; $\alpha = |\eta_0|^2/(2\kappa^2)$. The left satellite at $\Delta_p = 0$ has a classical amplitude $|\eta_0|^2/(4\kappa^2)$.

The nonclassical spectrum for two waves in a diffraction minimum (Fig. 3c) is centered at $\tilde{\Delta}_p = g^2 N/\Delta_{0a}$, with components at $\Delta_p^q \approx 2g^2 q/\Delta_{0a}$, and is very broad, $\sigma_\omega = g^2\sqrt{N}/\Delta_{0a}$; $\alpha = |\eta_0|^2/\kappa^2$.

In the limit $\kappa \gg g^2/\Delta_{0a}$, the integral expressions similar to Eq. (6) have the same parameters as for $\kappa < g^2/\Delta_{0a}$. For two modes in a diffraction minimum the photon number (Fig. 3d) is

$$\langle a_1^\dagger a_1 \rangle_{\rm SF} = \frac{|\eta_0|^2}{\sqrt{2\pi}\sigma_\omega} \int_{-\infty}^{\infty} \frac{\omega^2 e^{-\omega^2/2\sigma_\omega^2} d\omega}{(\Delta_p'^2 - \omega^2 - \kappa^2)^2 + 4\kappa^2\Delta_p'^2},$$

where $\Delta_p' = \Delta_p - \tilde{\Delta}_p$, while in a maximum (Fig. 3b)

$$\langle a_1^\dagger a_1 \rangle_{\rm SF} = \frac{|\eta_0|^2}{4\sqrt{2\pi}\sigma_\omega} \int_{0}^{\infty} \frac{\omega^2 e^{-(\omega - \tilde{\Delta}_p)^2/2\sigma_\omega^2} d\omega}{[\Delta_p(\Delta_p - \omega) + \kappa^2]^2 + \kappa^2\omega^2}.$$

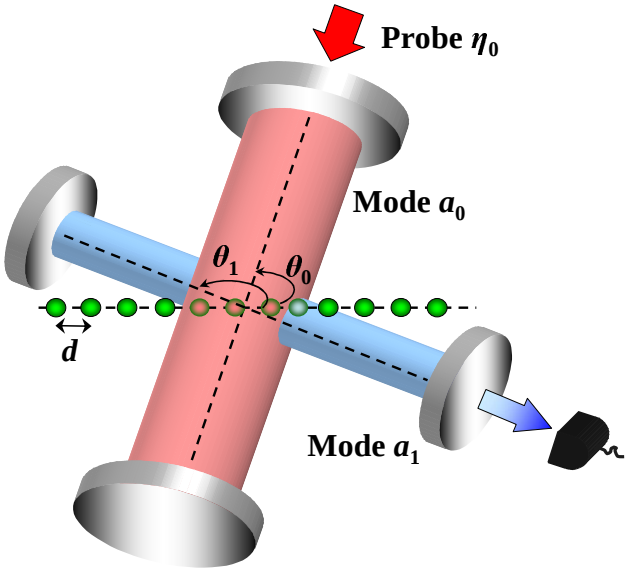

FIG. 1: **Schematic setup.** Atoms are periodically trapped in an optical lattice created by laser beams, which are not shown in this figure. Additionally, the atoms are illuminated by two light modes at the angles $\theta_{0,1}$ with respect to the lattice axis.

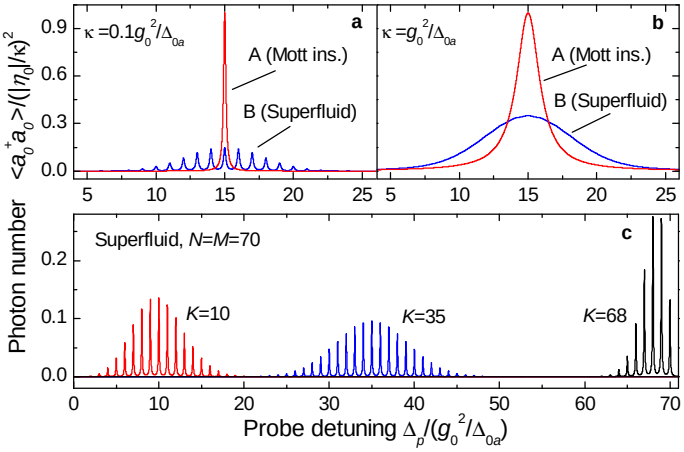

FIG. 2: **Photon number in a single cavity mode. a,** Single Lorentzian for MI (curve A) and many Lorentzians for SF (curve B), $\kappa = 0.1g^2/\Delta_{0a}$, $N = M = 30$, $K = 15$. **b,** The same as in **a** but $\kappa = g^2/\Delta_{0a}$ gives broadened contour for SF. **c,** Spectra for SF with $N = M = 70$ and different number of sites illuminated $K = 10, 35, 68$, $\kappa = 0.05g^2/\Delta_{0a}$.

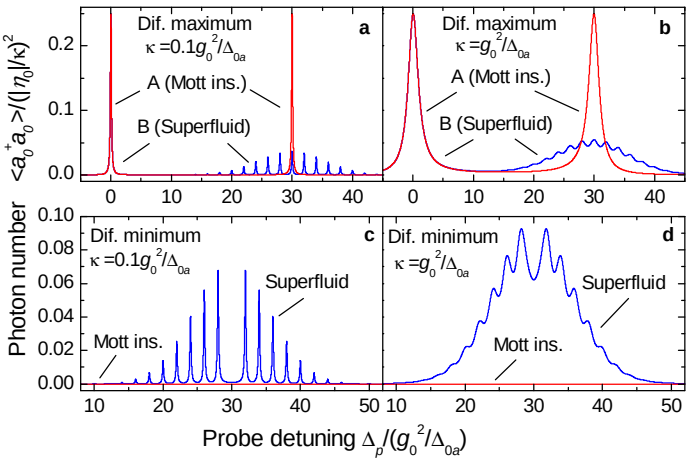

FIG. 3: **Photon number in one of two strongly coupled modes. a,** Diffraction maximum, doublet for MI (curve A) and spectrum with structured right satellite for SF (curve B), $\kappa = 0.1g^2/\Delta_{0a}$, $K = 15$. **b,** The same as in **a** but $\kappa = g^2/\Delta_{0a}$ gives broadened satellite for SF. **c,** Diffraction minimum, zero field for MI and structured spectrum for SF, $\kappa = 0.1g^2/\Delta_{0a}$, $K = 30$. **d,** The same as in **c** but $\kappa = g^2/\Delta_{0a}$ gives broadened contour for SF. $N = M = 30$ in all figures.